On the viscous destabilization of longshore currents

Uday Putrevu[1] A.M.ASCE, James T. Kirby[2] M.ASCE, Joan Oltman-Shay[3], and H. Tuba Özkan-Haller[4] A.M.ASCE

ABSTRACT: *The effects of lateral mixing on the stability of longshore currents are examined. For the model problem originally considered by Bowen and Holman (1989), it is shown that the inclusion of lateral mixing changes the stability characteristics of the longshore current. In particular, it eliminates the low wavenumber cutoff predicted by the inviscid theory.*

INTRODUCTION

In this paper we investigate how lateral mixing affects the stability of longshore currents. Bowen and Holman (1989; BH89 hereafter) showed that longshore currents in the surf zone are frequently unstable and that these instabilities manifest themselves as wavelike oscillations of the longshore current of the kind found by Oltman-Shay *et al.* (1989).

BH89 derived the equations governing the linear stability of the longshore current in the absence of bottom friction and lateral mixing. They showed that the stability of the longshore current is governed by a modified Rayleigh equation. BH89 solved the stability equation for a model problem in which a longshore current of the form sketched in figure 1 flows over a horizontal bottom. They demonstrated that the longshore current is unstable for wavenumbers in a certain range and that many properties of the waves generated due to the instability of the longshore current are consistent with the observations of shear waves reported by Oltman-Shay *et al.* (1989).

Since the pioneering work of Bowen and Holman, several contributions have been made that have clarified many aspects of the shear wave generation problem [see Özkan-Haller and Kirby (1998) for a brief review]. Here we consider how the inclusion of lateral mixing affects the stability of longshore currents.

[1]Research Scientist, NorthWest Research Associates, Inc., 14508 NE 20th Street, Bellevue, WA 98007, USA.

[2]Professor, Center for Applied Coastal Research, University of Delaware, Newark, DE 19716, USA.

[3]Senior Research Scientist, NorthWest Research Associates, Inc., 14508 NE 20th Street, Bellevue, WA 98007, USA.

[4]Assistant Professor, Department of Naval Architecture and Marine Engineering, University of Michigan, Ann Arbor, MI 48109, USA.

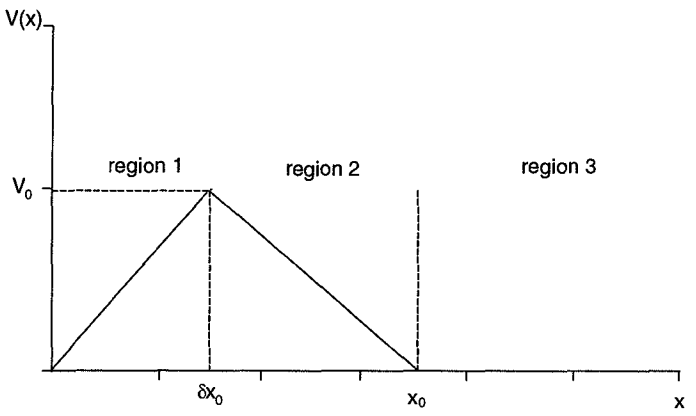

Figure 1: Velocity profile used by BH89. This same velocity profile is also used in our model problem. In all of the calculations below, we use $x_0 = 100$ m and $V_0 = 1$ m/s.

Falqués and Iranzo (1994) and Falqués *et al.* (1994) have already included lateral mixing in the calculations of the stability of longshore currents. Our work differs from that of Falqués *et al.* in that here we consider how the inclusion of lateral mixing changes the stability of a simple longshore current profile of the type considered by BH89. The simplicity of the current profile allows us to perform analytical calculations of how the addition of the lateral mixing changes the stability characteristics of the longshore current. This, in turn, makes the interpretation of the results easier.

The outline of the rest of the paper is as follows. We first derive the equation that governs the stability of the longshore current in the presence of lateral mixing. We then solve the resulting equation for the model problem considered by BH89. Example results are then presented that demonstrate that the inclusion of lateral mixing can destabilize the longshore current. A discussion of the mechanism by which lateral mixing can destabilize the longshore current follows the example results. The paper concludes with a summary.

MATHEMATICAL FORMULATION

We start with the depth-integrated equations of continuity and momentum

$$\frac{\partial \zeta}{\partial t} + \frac{\partial (h+\zeta) u_i}{\partial x_i} = 0 \tag{1}$$

$$\frac{\partial u_i}{\partial t} + u_j \frac{\partial u_i}{\partial x_j} = -g \frac{\partial \zeta}{\partial x_i} + \frac{1}{\rho h} \frac{\partial S_{ij}}{\partial x_j} + \frac{\partial}{\partial x_j} \left[\nu h \left(\frac{\partial u_i}{\partial x_j} + \frac{\partial u_j}{\partial x_i} \right) \right] - \frac{\tau_{b,i}}{\rho h} \tag{2}$$

where ζ is the surface elevation, h is the water depth, u_i is the depth-integrated horizontal velocity, S_{ij} is the radiation stress, ν is a lateral mixing coefficient, and

$\tau_{b,i}$ is the bottom shear stress. The lateral mixing represented by the ν terms in (2) could be either due to turbulent lateral mixing (generated by breaking waves) or due to dispersive mixing generated by the interaction of the cross-shore and longshore currents (Svendsen and Putrevu 1994; Smith 1997). Since these lateral mixing terms have the same form as viscous terms, the terms *viscosity* and *lateral mixing* will be used interchangeably in the rest of this paper.

We now assume that the total flow consists of a steady longshore current $V(x)$ and a shear wave with surface elevation $\eta(x,y,t)$ and depth-averaged horizontal velocities $u(x,y,t)$ and $v(x,y,t)$ in the cross-shore (x) and longshore (y) directions. We further assume that u and v are much smaller than V. Under these assumptions the momentum equations governing the shear wave reduce to (neglecting the forcing and the bottom shear stress)

$$\frac{\partial u}{\partial t}+V\frac{\partial u}{\partial y}=-g\frac{\partial \eta}{\partial x}+\frac{2}{h}\frac{\partial}{\partial x}\left(\nu h\frac{\partial u}{\partial x}\right)+\frac{1}{h}\frac{\partial}{\partial y}\left[\nu h\left(\frac{\partial u}{\partial y}+\frac{\partial v}{\partial x}\right)\right] \tag{3}$$

$$\frac{\partial v}{\partial t}+u\frac{dV}{dx}+V\frac{\partial v}{\partial y}=-g\frac{\partial \eta}{\partial y}+\frac{2}{h}\frac{\partial}{\partial y}\left(\nu h\frac{\partial v}{\partial y}\right)+\frac{1}{h}\frac{\partial}{\partial x}\left[\nu h\left(\frac{\partial u}{\partial y}+\frac{\partial v}{\partial x}\right)\right] \tag{4}$$

The continuity equation under the rigid lid assumption [see BH89 or Dodd and Thornton (1990) for a justification of the rigid lid assumption] reduces to

$$\frac{\partial}{\partial x}(hu)+\frac{\partial}{\partial y}(hv)=0 \tag{5}$$

The nondivergence of the continuity equation allows us to introduce a stream function Ψ such that

$$\Psi_x=hv \qquad \Psi_y=-hu \tag{6}$$

Since we are seeking wavelike solutions, we assume that

$$\Psi(x,y,t)=\phi(x)\exp i(ky-\omega t) \tag{7}$$

where k is the wavenumber and ω is the frequency. The stream function can be used to combine (3) and (4) [by cross-differentiation followed by subtraction] into a single equation in ϕ:

$$\begin{aligned}(V-c)\left[\left(\frac{\phi_x}{h}\right)_x-\frac{k^2\phi}{h}\right]-\phi\left(\frac{V_x}{h}\right)_x&=\frac{\nu}{ik}\left(\frac{\partial^2}{\partial x^2}-k^2\right)\left[\left(\frac{\phi_x}{h}\right)_x-\frac{k^2\phi}{h}\right]\\ +\frac{1}{ik}\left\{\nu_x\left[\left(\frac{\phi_x}{h}\right)_{xx}-\frac{k^2\phi_x}{h}-\frac{k^2\phi h_x}{h^2}\right]+\left[\frac{(\nu h)_x}{h}\left(\frac{\phi_x}{h}\right)_x\right]_x-\frac{k^2(\nu h)_x}{h}\left(\frac{\phi}{h}\right)_x\right\}&\end{aligned} \tag{8}$$

where $c=\omega/k$ is the wave speed. The boundary conditions corresponding to (8) are

$$\phi,\frac{d\phi}{dx}=0 \quad x=0,x\to\infty \tag{9}$$

(8) subject to (9) forms an eigenvalue problem. As is usual in stability calculations, we assume that the wavenumber k is known and treat the frequency ω as the eigenvalue.

If ω has a positive imaginary component for a given k it implies that the longshore current is unstable to disturbances of that wavenumber.

The terms on the RHS of (8) are terms that arise due to the inclusion of the lateral mixing. For $\nu = 0$, (8) reduces to the equation derived by BH89. [The appropriate boundary conditions for the reduced equation are $\phi = 0$ at $x = 0, x \to \infty$.] For small values of ν the RHS of (8) is small and unimportant except at the shoreline and the singular points of the inviscid equation. At the shoreline, the necessity of satisfying an additional boundary condition leads to the generation of a boundary layer. At the locations where $V = c$, the inviscid equation is, in general, singular whereas the full equation is not. Therefore, at these locations, internal boundary layers will develop when lateral mixing is included.

MODEL PROBLEM

We consider the stability of the longshore current sketched in Figure 1. The bottom is assumed to be horizontal. The inviscid stability of this current profile was calculated by BH89. Here we modify their solution to account for lateral mixing. For a horizontal bottom (8) reduces to the Orr-Sommerfeld equation

$$(V-c)\left(\frac{d^2}{dx^2}-k^2\right)\phi - V_{xx}\phi = \frac{\nu}{ik}\left(\frac{d^2}{dx^2}-k^2\right)^2\phi \tag{10}$$

We assume that the strength of the lateral mixing is such that a typical term on the RHS of (10) is much smaller than a typical term on the LHS. Formally, this requires that

$$\frac{k_t \nu_t}{V_0} \ll 1 \tag{11}$$

where k_t is a typical wavenumber, ν_t is a typical value of the lateral mixing coefficient, and V_0 is the maximum longshore current. Note that since $k_t \sim 0.01$ m^{-1}, $\nu_t \sim 0.1$ m^2/s, $V_0 \sim 1$ m/s, (11) is easily satisfied.

For the longshore current sketched in figure 1, (10) reduces to

$$(V-c)\left(\frac{d^2}{dx^2}-k^2\right)\phi = \frac{\nu}{ik}\left(\frac{d^2}{dx^2}-k^2\right)^2\phi \tag{12}$$

in each of the three regions. In this case, the singular points of the inviscid equation are the points $x = \delta x_0$ and $x = x_0$ and internal boundary layers develop at these points to smooth out the discontinuities predicted by the inviscid theory.

At $x = 0$ and $x = x_0$, the boundary layer correction to the inviscid solution is governed approximately by

$$-c\frac{d^2\phi_{BL}}{dx^2} \approx \frac{\nu}{ik}\frac{d^4\phi_{BL}}{dx^4} \tag{13}$$

which implies that at these locations

$$\phi_{BL} \propto \exp\left[\pm(1-i)\beta_1 x\right] \tag{14}$$

where $\beta_1 = \sqrt{\omega/2\nu} \gg k$. At $x = \delta x_0$ the boundary layer correction is approximately governed by

$$(V_0-c)\frac{d^2\phi_{BL}}{dx^2} \approx \frac{\nu}{ik}\frac{d^4\phi_{BL}}{dx^4} \tag{15}$$

which leads to

$$\phi_{BL} \propto \exp\left[\pm(1+i)\beta_2 x\right] \tag{16}$$

where $\beta_2 = \sqrt{(kV_0 - \omega)/2\nu} \gg k$.

The solution to (12) can therefore be written as

$$\phi = \begin{cases} \sinh(kx) + B_1\cosh(kx) + F_1\exp[-(1-i)\beta_1 x] \\ \quad +G_1\exp[(1+i)\beta_2(x-\delta x_0)] & x < \delta x_0 \\ \\ A_2\sinh[k(x-\delta x_0)] + B_2\cosh[k(x-\delta x_0)] \\ \quad +F_2\exp[-(1+i)\beta_2(x-\delta x_0)] + G_2\exp[(1-i)\beta_1(x-x_0)] & \delta x_0 < x < x_0 \\ \\ A_3\exp[-k(x-x_0)] + F_3\exp[-(1-i)\beta_1(x-x_0)] & x > x_0 \end{cases} \tag{17}$$

The unknown coefficients (the A's, B's, F's, and G's) and the eigenvalue (ω) have to be determined by imposing the boundary conditions at $x = 0$ and the matching conditions at $x = \delta x_0$ and $x = x_0$. [The boundary conditions at infinity have already been imposed in (17).] The appropriate matching conditions are:

1. hu continuous $\Rightarrow$ ϕ continuous
2. hv continuous $\Rightarrow$ ϕ_x continuous
3. η continuous $\Rightarrow$ $ik\phi dV/dx + \nu d^3\phi/dx^3$ continuous
4. $-g\partial\eta/\partial x + \nu\partial^2 u/\partial x^2$ continuous $\Rightarrow$ $(V-c)d^2\phi/dx^2 + (\nu/ik)[2k^2 d^2\phi/dx^2 - d^4\phi/dx^4]$ continuous

The last of these conditions follows from the cross-shore momentum equation (3).

Applying the boundary and matching conditions leads to (after a fair amount of algebra)

$$\omega^2 + F(\delta, kx_0)\omega + G(\delta, kx_0) + \left(\frac{k}{\beta_1}\right) T(\omega, kx_0, \delta, \beta_1/\beta_2) = O\left(\frac{k}{\beta}\right)^2 \tag{18}$$

where

$$F = -kV_0\left[1 - \frac{S_0}{(S_0+C_0)}\frac{V_{x2}}{kV_0} - \frac{(S_{1-\delta}+C_{1-\delta})S_\delta}{(S_0+C_0)}\frac{\Delta V_x}{kV_0}\right] \tag{19}$$

$$G = (kV_0)^2\left[\frac{V_{x2}\Delta V_x}{(kV_0)^2}\frac{S_\delta S_{1-\delta}}{(S_0+C_0)} - \frac{S_0}{(S_0+C_0)}\frac{V_{x2}}{kV_0}\right] \tag{20}$$

$$\begin{aligned} T = {} & \left\{2(1+i)\left\{\sigma\left[C_0 + \frac{\omega}{V_{x2}}(S_0+C_0)\right] + \Delta V_x C_\delta\left[S_{1-\delta} + \frac{\omega}{V_{x2}}(S_{1-\delta}+C_{1-\delta})\right]\right\}\right. \\ & +\sigma(1+i)\left[(S_0+C_0) + S_\delta\frac{\Delta V_x}{\sigma}(S_{1-\delta}+C_{1-\delta})\right] \\ & \left.-\frac{\beta_1}{\beta_2}\frac{(\Delta V_x)^2}{\sigma}(1-i)S_\delta\left[S_{1-\delta} + \frac{\omega}{V_{x2}}(S_{1-\delta}+C_{1-\delta})\right]\right\}\frac{V_{x2}}{4(S_0+C_0)} \end{aligned} \tag{21}$$

In the above, $S_0 = \sinh(kx_0)$, $S_\delta = \sinh(k\delta x_0)$, $S_{1-\delta} = \sinh[kx_0(1-\delta)]$ and the C's are short forms for the corresponding cosh functions. Additionally, V_{x1} and V_{x2} represent dV/dx in regions 1 and 2 respectively, $\Delta V_x = V_{x1} - V_{x2}$, and $\sigma = \omega - kV_0$.

In the limit of $\nu \to 0$ ($\beta_1, \beta_2 \to \infty$), F and G reduce to the expressions given by BH89's (16), and we then recover Bowen and Holman's solution. The term denoted by T represents the effects of including the lateral mixing.

For $\nu = 0$, (18) has two solutions for ω for a given value of k – these are the solutions found by BH89. For small ν, the T-term modifies these solutions. These modifications can be calculated in a straightforward manner. In addition to modifying the BH89 solution, the T-term also introduces new roots to (18). The significance of these new roots is, at present, unknown. In the following, we discuss only the roots that can be interpreted as modifications of the BH89 solution.

RESULTS

Figure 2 shows the variation of the growth rate ω_{im} as a function of the wave number. For comparison, we also show Bowen and Holman's inviscid solution. It is clear from this figure that including lateral mixing in the calculations significantly alters the stability characteristics. In particular, the range of wavenumbers over which the instability occurs is significantly enhanced, the location of the most unstable wave is changed, and the low wavenumber cutoff predicted by the inviscid theory is removed.

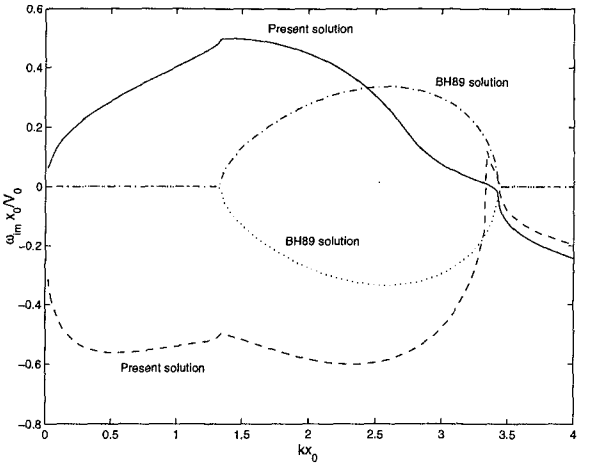

Figure 2: Plot of growth rate, ω_{im}, vs wavenumber for the model problem. The parameters used in this calculation are $\delta = 0.5$, $\nu = 5 \times 10^{-3}$ m^2/s, $x_0 = 100$ m, and $V_0 = 1$ m/s.

In a recent paper, Shrira *et al.* (1997) solved the weakly nonlinear version of the model problem considered by BH89. They showed that the triad interactions between individual shear wave modes could remove the low wavenumber cutoff predicted by the linear inviscid theory. Our results show that including the lateral mixing leads to

the same result. Thus, a plausible scenario is that the low wavenumber oscillations are initially generated by the present mechanism and grow to finite amplitude by the mechanism discussed by Shrira *et al.*

Figure 3 shows the variation of the real part of the frequency as a function of the wavenumber for the branches of the solution that have a positive growth rate. We see from this figure that the addition of lateral mixing does not alter the dispersion relationship significantly in the region where the inviscid theory predicts an instability.

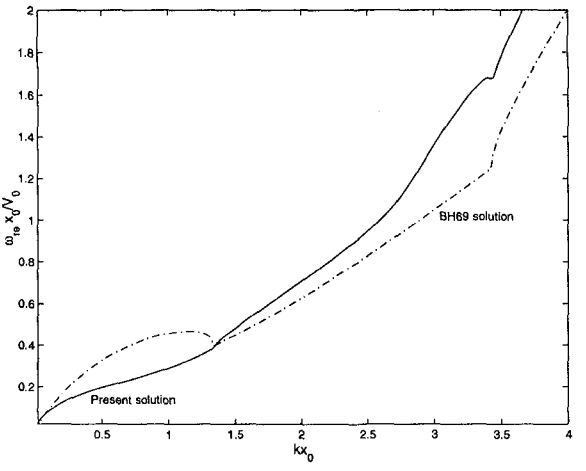

Figure 3: Plot of the real part of the frequency, ω_{re}, vs wavenumber for the model problem. The parameters used in this calculation are $\delta = 0.5$, $\nu = 5 \times 10^{-3}$ m^2/s, $x_0 = 100$ m, and $V_0 = 1$ m/s. Note that only the branches that have a positive growth rates are shown.

Figure 2 showed the growth rate as a function of wavenumber for a particular choice of the lateral mixing coefficient ν. It is also of interest to examine the sensitivity of the growth rate at a fixed wavenumber to the choice of the mixing coefficient. This is done in figure 4 which shows the variation of the growth rate as a function of ν. Realistic values of ν for the nearshore are expected to be in the range 10^{-3} to 0.1 m^2/s. The lower end of the range would apply if the lateral mixing were due to the turbulence generated by breaking waves (Svendsen 1987; George *et al.* 1994). The higher end would apply if, as is more likely, the lateral mixing were due to dispersive mixing generated by the interaction of the cross-shore and longshore currents (Svendsen and Putrevu 1994). We see from figure 4 that the growth rate increases with ν for ν in the range that is normally expected.

BH89 found that the backshear parameter δ controls the strength of the instability in

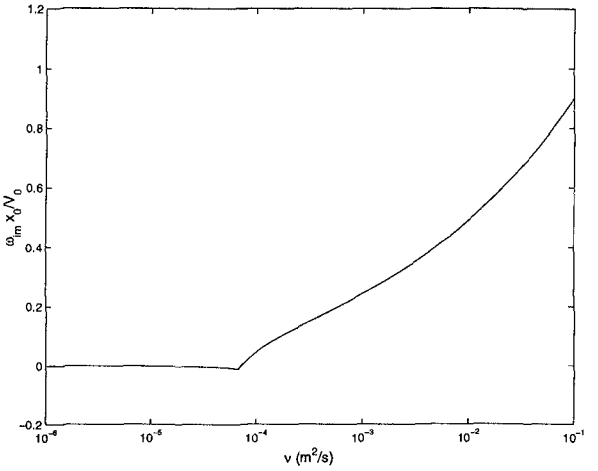

Figure 4: Variation of growth rate with the lateral mixing coefficient. The parameters used in this calculation are $\delta = 0.5$, $kx_0 = 1$, $x_0 = 100$ m, and $V_0 = 1$ m/s.

the inviscid problem – the stronger the backshear, the stronger is the instability. It is therefore of interest to see whether this behavior carries over to the case where lateral mixing is included. Figure 5 shows the variation of the growth rate with δ. For this calculation we have chosen the parameters such that the inviscid calculations predict stability. This figure clearly shows that the backshear δ also controls the stability of the viscous problem.

MECHANISM

The calculations presented so far have shown that including the lateral mixing can destabilize an otherwise stable longshore current. Since this result is somewhat counter-intuitive, it is useful to examine it in more detail. Therefore, we discuss below the mechanism by which lateral mixing (or viscosity) can destabilize a longshore current. The discussion here largely follows Lin's (1967) discussion (see pp. 60-63 of Lin's book).

For h = constant, the equations governing the stability of the longshore current reduce to

$$\frac{\partial u}{\partial x} + \frac{\partial v}{\partial y} = 0 \tag{22}$$

$$\frac{\partial u}{\partial t} + V\frac{\partial u}{\partial y} = -g\frac{\partial \eta}{\partial x} + \nu\left(\frac{\partial^2 u}{\partial x^2} + \frac{\partial^2 u}{\partial y^2}\right) \tag{23}$$

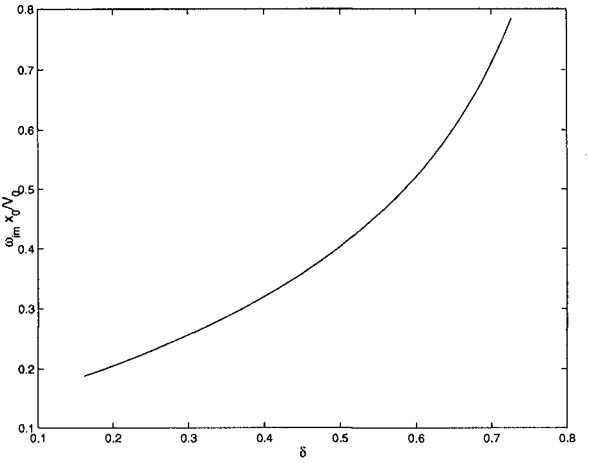

Figure 5: Variation of the growth rate as a function of the backshear parameter. The values used in the calculations are $\nu = 5 \times 10^{-3}$, m^2/s and $kx_0 = 1$, $x_0 = 100$ m, and $V_0 = 1$ m/s. The inviscid solution is stable for this choice of parameter values.

$$\frac{\partial v}{\partial t} + u\frac{dV}{dx} + V\frac{\partial v}{\partial y} = -g\frac{\partial \eta}{\partial y} + \nu\left(\frac{\partial^2 v}{\partial x^2} + \frac{\partial^2 v}{\partial y^2}\right) \tag{24}$$

From these equations, it is straightforward to derive the following energy equation

$$\begin{aligned}\frac{dE}{dt} &= -\int_0^\infty h\overline{uv}(dV/dx)dx \\ &\quad -\nu\int_0^\infty h\left[(\partial u/\partial x)^2 + (\partial u/\partial y)^2 + (\partial v/\partial x)^2 + (\partial v/\partial y)^2\right]dx\end{aligned} \tag{25}$$

where an overbar denotes averaging over a shear wave period and E is the total kinetic energy defined by

$$E = \frac{h}{2}\int_0^\infty \overline{(u^2+v^2)}dx \tag{26}$$

(Because of the rigid-lid assumption, the potential energy does not enter the energy equation.)

The first term in (25) represents the energy transfer from the longshore current to the shear wave and the second term represents the dissipation of the shear wave energy by the viscosity-like terms. Now the introduction of viscosity changes the phase between the cross-shore and longshore velocities so that the first term on the RHS of (25) is

changed relative to the inviscid solution. Thus, viscous terms modify the inviscid solution in two important ways: 1) they change the phase between the velocity components of the shear wave which leads to an extraction of energy from the longshore current and 2) they lead to direct dissipation of the shear wave energy. Therefore, viscous terms can destabilize an otherwise stable longshore current profile if the energy extracted from the longshore current exceeds the direct dissipation.

To explore the changes caused by the inclusion of viscosity-like terms further, we show in figures 6, 7, and 8 the cross-shore variations of ϕ (which is proportional to u), ϕ_x (proportional to v), and $-\overline{uv}(dV/dx)$ respectively. (The parameter values are chosen such that the inviscid calculation predicts stability whereas the viscous calculation predicts instability.) It is clear from figures 6 and 7 that the introduction of lateral mixing terms changes the phase of u and v. Figure 8 shows that this change in phase results in an extraction of energy from the longshore current. Figure 8 further demonstrates that most of the energy extraction takes place on the seaward face of the longshore current, thereby explaining the importance of the backshear on the stability found in figure 5.

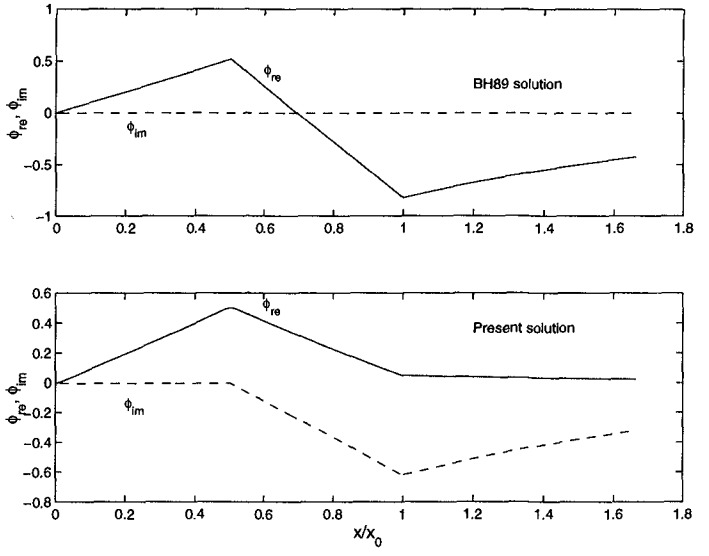

Figure 6: Cross-shore variation of $\phi \propto u$. Top panel inviscid (BH89) solution. Bottom panel calculation including lateral mixing terms. Note that the scale of the y axis is arbitrary. The parameter values used in the calculations are $kx_0 = 1$, $x_0 = 100$ m, $\delta = 0.5$, $V_0 = 1$ m/s, and $\nu = 5 \times 10^{-3}$ m^2/s.

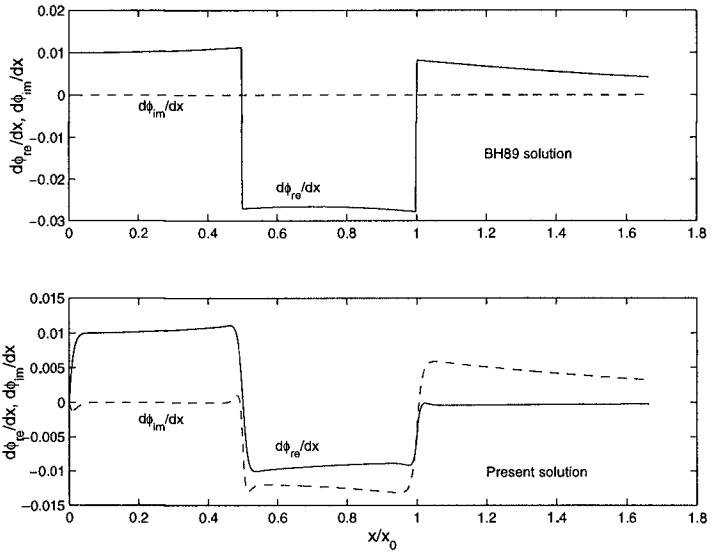

Figure 7: Cross-shore variation of $\phi_x \propto v$. Top panel inviscid (BH89) solution. Bottom panel calculation including lateral mixing terms. Note that the scale of the y axis is arbitrary. The parameter values used in the calculations are $kx_0 = 1$, $x_0 = 100$ m, $\delta = 0.5$, $V_0 = 1$ m/s, and $\nu = 5 \times 10^{-3}$ m^2/s.

SUMMARY

In this paper we considered how the addition of lateral mixing affects the stability of longshore currents. We showed that the inclusion of lateral mixing can destabilize an otherwise stable longshore current. The instability induced by the lateral mixing is such that it removes the low-wavenumber, low-frequency cutoff predicted by the inviscid theory. As in the inviscid case, the parameter that controls the stability of the longshore current is the shear on the seaward face of the longshore current.

The inclusion of lateral mixing destabilizes the longshore current as follows: it provides a Reynolds' stress that enables the shear wave to extract energy from the longshore current. We showed that this extraction of energy takes place mainly on the seaward face of the longshore current.

Finally, note that Falqués and Iranzo (1994) and Falqués *et al.* (1994) have already investigated the effects of lateral mixing on the stability of longshore currents using a numerical model. While Falqués *et al.* did find that the inclusion of lateral mixing increased the instability in certain cases, they did not find the instability at low

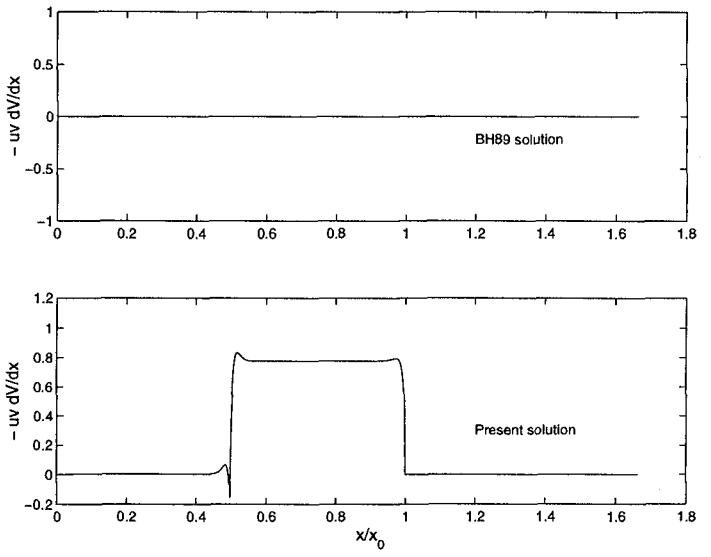

Figure 8: Cross-shore variation of $-\overline{uv}dV/dx$. Top panel inviscid (BH89) solution. [The inviscid solution is stable for the choice of parameter values used in this calculation (see below). This is the reason why $\overline{uv}$ is zero for the BH89 solution.] Bottom panel calculation including lateral mixing terms. Note that the scale of the y axis is arbitrary. The parameter values used in the calculations are $kx_0 = 1$, $x_0 = 100$ m, $\delta = 0.5$, $V_0 = 1$ m/s, and $\nu = 5 \times 10^{-3}$ m^2/s.

wavenumbers found here. At present we do not know whether this discrepancy is due to the artificial nature of our model problem or due to the boundary conditions used by Falqués *et al.* Therefore, it is necessary to extend the present analysis to more realistic longshore current variations.

ACKNOWLEDGEMENTS

This work was sponsored by the U.S. Office of Naval Research, Coastal Dynamics Program under contracts N00014-97-C-0075 (UP and JOS), N00014-94-1-0214 and N00014-98-1-0521 (JTK and TOH).

REFERENCES

Bowen, A. J. and R. A. Holman, 1989. Shear instabilities in the mean longshore current 1: Theory. *J. Geophys. Res.*, **94**: 18,023-030.

Dodd, N. and E. B. Thorntón, 1990. Growth and energetics of shear waves in the nearshore. *J. Geophys. Res.*, **95**, 16,075-083.

Falqués, A. and V. Iranzo, 1994. Numerical simulation of vorticity waves in the nearshore. *J. Geophys. Res.*, **99**, 825-841.

Falqués, A., V. Iranzo and M. Caballeria, 1994. Shear instability of longshore current: Effects of dissipation and nonlinearity. *Proc. Intl. Conf. Coastal Eng.*, **24**, 1983-1997.

George, R., R. E. Flick and R. T. Guza, 1994. Observations of turbulence in the surf-zone. *J. Geophys. Res.*, **99**, 801-810.

Lin, C. C., 1967. *Theory of hydrodynamic stability.* Cambridge University Press, 155 pp.

Oltman-Shay, J., P. A. Howd and W. A. Berkemeier, 1989. Shear instabilities of the mean longshore current 2: Field observations. *J. Geophys. Res.*, **94**, 18031-18042.

Özkan-Haller, H. T. and J. T. Kirby, 1998. Nonlinear evolution of shear instabilities of the longshore current: A comparison of observations and computations *J. Geophys. Res.*, in press.

Shrira, V. I., V. V. Vornovich, and N. G. Kozhelupova, 1997. Explosive instability of vorticity waves. *J. Phys. Oceanogr.*, **27**, 542-554.

Smith, R., 1997. Multi-mode models of flow and of solute dispersion in shallow water. Part 3. Horizontal dispersion tensor for the velocity, *J. Fluid Mech.*, **352**, 331-340.

Svendsen, I. A. 1987. Analysis of surf zone turbulence. *J. Geophys. Res.*, **92**, pp. 5115-24.

Svendsen, I.A. and U. Putrevu, 1994. Nearshore mixing and dispersion. *Proc. Roy. Soc. Lond. A.*, **445**, 561-576.